Quantum Electronics **29** (1) 65 – 68 (1999)

PACS numbers: 42.81.Dp; 42.40.Eq; 42.65.Hw

Properties of the cladding modes of an optical fibre excited by refractive-index gratings

S A Vasil'ev ¶, E M Dianov, O I Medvedkov, V N Protopopov,
D M Costantini, A Iocco, H G Limberger, R P Salathe

Abstract. The properties of the cladding modes of an optical fibre, excited by photoinduced long-period fibre gratings, were investigated by the near- and far-field methods. It is shown that the cladding modes considered are of the HE_{1m} type. A satisfactory agreement between the experimental and calculated distributions of the electromagnetic field of the modes is demonstrated. It was found that the propagation length of a cladding mode in the unperturbed fibre reaches 1 m.

1. Introduction

Refractive index (RI) gratings, induced in the core of an optical fibre by UV radiation, have found a multiplicity of applications in fibre-optic devices, such as various types of fibre lasers, optical multiplexers and demultiplexers, dispersion compensators, fibre sensors of physical quantities, etc. [1]. Several types of RI gratings have now been proposed and are actually used in practical applications. Bragg gratings [2], ensuring resonant coupling of the fundamental mode of the fibre core to the same mode propagating in the opposite direction, as well as long-period gratings [3], coupling the core mode to the cladding modes propagating in the same direction, are the most popular. The cladding modes are manifested also in Bragg gratings with a high coupling coefficient, leading as a rule to undesirable absorption on the short-wavelength side relative to the main resonance [4].

Despite extensive applications of fibre gratings, the properties of cladding modes have so far been inadequately investigated. Several communications have been devoted to the numerical modelling of the distribution of their fields [5, 6], but the results of these studies have not been confirmed experimentally. The experimentally measured fields of cladding modes reported recently [7] have not been duly accounted for and the proposed interpretation of the types of excited cladding modes does not agree with the classification proposed for them [5, 6] and seems unconvincing. We may also note that even in a theoretical consideration of the type of cladding modes excited by long-period gratings, one encounters alternative interpretations which require elucidation. Thus, the HE_{1m} and EH_{1n} cladding modes have combined [6] in a single series, which is convenient in numerical calculations, although in our view it complicates the interpretation of the radial mode number.

Apart from refining the type of cladding modes excited by fibre RI gratings, it is of interest to investigate their propagation length after excitation and to discover the factors limiting this length. The mode propagation length is an important parameter, particularly in the fabrication of long gratings and devices in which reverse energy transfer from a cladding mode to a core mode is employed [8, 9]. We may also note that long-period gratings constitute an ideal means for the selective excitation of one cladding mode in a significantly multimode fibre structure, which is again of interest for practical applications.

This communication reports an experimental investigation of the distribution of the fields of fibre cladding modes excited by long-period fibre RI gratings. The study was performed by the near- and far-field methods. In order to eliminate the alternative interpretations encountered in the literature on the question of the classification of grating-excited cladding modes, attention was concentrated on a comparison of the experimental results with calculated data. The propagation length of a selected cladding mode and the influence of the method of securing a fibre segment, located ahead of a grating, on this parameter were investigated qualitatively.

2. Experimental results and their analysis

The long-period gratings employed in our experiments were formed in a single-mode germanosilicate fibre with a step RI profile, a numerical aperture of 0.23, and core and cladding diameters of 3.5 and 125 μm, respectively. The fibre was exposed to the radiation from an excimer ArF laser ($\lambda = 193$ nm, energy density ~ 100 mJ cm^{-2}, pulse repetition frequency $f \approx 20$ Hz, exposure time $t \approx 3$ min) through an amplitude mask with a period of 200 μm. The period of the grating formed in the fibre was varied in the range 200 – 300 μm by varying the direction of the mask lines relative to the fibre axis. The grating length was ~ 20 mm. A typical transmission spectrum of the grating with identification of the orders m of the coupled cladding modes is presented in Fig. 1.

A semiconductor laser tunable in the range 1.46 – 1.6 μm and with a power in the fibre core of about 1 mW was used to record the transmission spectra of the gratings and in the analysis of the cladding modes. Variation of the grating

¶ In the Western literature this author's name is sometimes spelt Vasiliev.

S A Vasil'ev, E M Dianov, O I Medvedkov, V N Protopopov Fibre Optics Centre at the Institute of General Physics, Russian Academy of Sciences, ul. Vavilova 38, 117756 Moscow, Russia;
D M Costantini, A Iocco, H G Limberger, R P Salathe Institute of Applied Optics, Swiss Federal Institute of Technology, CH-1015 Lausanne, Switzerland

Received 18 September 1998
Kvantovaya Elektronika **26** (1) 65 – 68 (1999)
Translated by A K Grzybowski

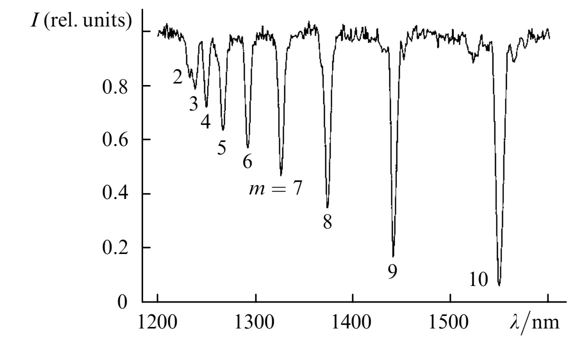

Figure 1. Typical transmission spectrum of a long-period grating. The numbers indicate the radial order m of the coupled cladding mode.

period made it possible to ensure that the wavelength of the resonant coupling of the fundamental mode with the first ten cladding modes was in the laser tuning range. In order to measure the distribution of the field of a cladding mode, the fibre was cleaved directly behind the grating. The lasing wavelength was chosen equal to the wavelength of the resonant coupling with a specific cladding mode. In order to avoid any kind of perturbations of a grating-excited cladding mode, the fibre was secured ahead of the grating in such a way that its free part contained the grating. The depth of the resonances investigated varied in the range 3 – 10 dB, so that an appreciable part of the power of the fundamental fibre mode passed through the grating and, as shown below, was taken into account in the interpretation of the results.

The distributions of the near and far fields were investigated with the aid of an IR camera, the signal from which was processed by a computer. A 20-fold objective was used in the analysis of the near field. An image of the fibre end-face magnified by a factor of approximately 50 was recorded by the camera. The far field was measured without using additional optical devices, at a distance of ~ 5 cm from the investigated end-face. The camera had an approximately linear response over the entire range of measurements with the exception of a relatively small region near saturation.

3. The near field

Fig. 2 illustrates the distributions of the near field obtained for a group of cladding modes. All the modes have a clear axial symmetry, which corresponds to the azimuthal number 1 and the number of rings is equal to the radial mode number m. In series of instances, presented in Fig. 2, the fundamental fibre mode field masks the inner rings of the cladding mode; at the same time, all the rings are clearly visible for certain distributions (Figs 2d and 2e). It is also essential to note that the white diffraction cross visible in the images arises as a consequence of the relatively high intensity of the fundamental mode and is not a part of the structure of the cladding modes. The substructure of the rings with a high spatial frequency (Fig. 2a) is apparently induced by the fact that, in the second order of the grating, a higher-order cladding mode is excited at the wavelength employed, in addition to the HE_{14} mode.

The experimental distributions presented permit a clear classification of the cladding modes excited by long-period gratings as type HE_{1m} ($m > 1$) modes [5]. These modes are linearly polarised and have the maximum overlap integral and hence the maximum coefficient of coupling to the

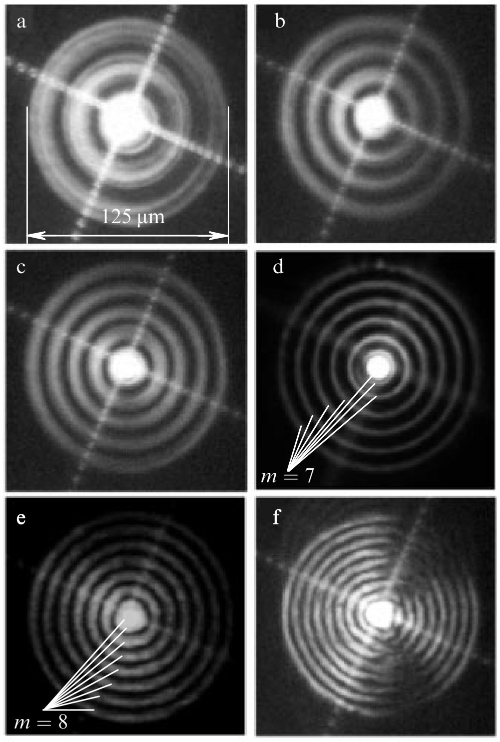

Figure 2. Intensity distributions in the near field for the modes HE_{1m} with $m = 4$ (a), 5 (b), 6 (c), 7 (d), 8 (e), and 10 (f).

fundamental mode, at least for relatively low radial numbers ($m < 10$), which are most often encountered in practice. The axially symmetric type EH_{1n} modes have a zero field along the fibre axis, so that the integral of the overlap of the fundamental mode with the latter becomes significant only for large radial numbers ($n > 10$) [6].

Fig. 3 presents the measured and calculated radial distributions of the far field intensities of the HE_{18} mode. The calculations were made on the assumption of a step RI profile of the fibre core by the method already described [5]. Evidently, the calculation agrees well with experiment in respect of the positions of the rings and their relative intensities, which constitute the structure of the mode. We shall only note that the central part of the measured radial distribution contains the partially transmitted fundamental mode

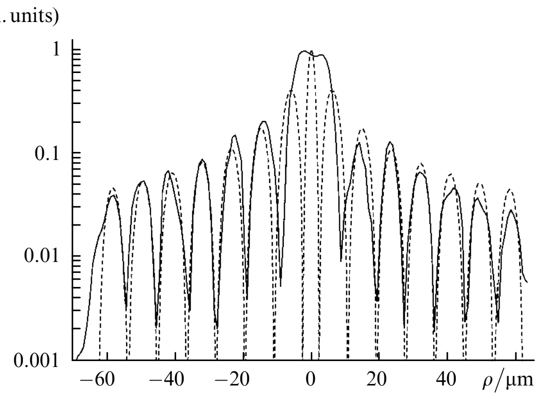

Figure 3. Experimentally determined (continuous curve) and calculated (dashed curve) radial intensity distributions in the near field for the mode HE_{18}.

and, furthermore, is in the saturation region of the camera. For these reasons, it is distorted.

4. The far field

Analysis of the distribution of the intensity in the far field of the radiation emerging from the end-face of the fibre waveguide can also be used to investigate the properties of cladding modes. The distribution of the electric field in the far zone $E_{\rm f}(r,\,\theta)$ is linked to the field in the fibre $E(\rho)$ by the Fourier transformation, which in the cylindrical symmetry case considered here assumes the form [10]

$$E_{\rm f}(r,\,\theta) = \frac{j}{\lambda r}\exp(-jkr)E_{\rm H}(q)\ , \qquad (1)$$

where

$$E_{\rm H}(q) = 2\pi\int_0^{\infty} E(\rho)J_0(2\pi q\rho)\rho\,{\rm d}\rho\,; \qquad q = \frac{\sin\theta}{\lambda}\,; \qquad k = \frac{2\pi}{\lambda}\,;$$

λ is the wavelength of the probe radiation.

Fig. 4 illustrates the distributions of the radiation intensity in the far field obtained on excitation of the cladding modes HE_{17} and HE_{18}. As in the near-field case, the far-field pattern is axially symmetric, but the radial distribution has no distinct characteristics. For example, the distribution for the mode HE_{17} (Fig. 4a) has a minimum intensity on the axis and one bright peripheral ring, whereas a local intensity maximum on the axis and two rings with approximately equal intensities on the periphery are observed in the distribution for the mode HE_{18} (Fig. 4b). Such behaviour can be explained by the presence, in the above distributions, of an appreciable fraction of the power of the fundamental mode.

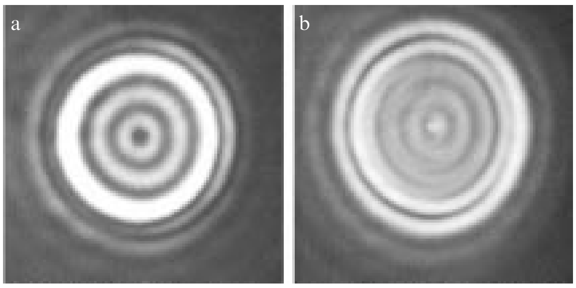

Figure 4. Intensity distributions in the far field for the modes HE_{17} (a) and HE_{18} (b).

Since the width of the far-field distribution for the fundamental mode is comparable with the width of the distribution for the cladding mode, it follows that, in order to obtain the far-field pattern, the amplitudes of the electric fields of the core and cladding modes must be added together taking into account the difference between their phases. Fig. 5 presents the angular distributions in the far field calculated using formula (1) for the modes HE_{11}, HE_{17}, and HE_{18} having equal intensities. The difference between the phases of the fundamental and cladding modes can evidently alter significantly the intensity distribution in the far field; for example, the intensity of the radiation of the cladding mode along the axis can be both increased and quenched by the core mode (Fig. 4). In the case under consideration, the difference between the phases of the fundamental and cladding modes depends on the parameters of the grating employed, the mode propagation constants, and the distance from the grating to the emitting end-face of the fibre.

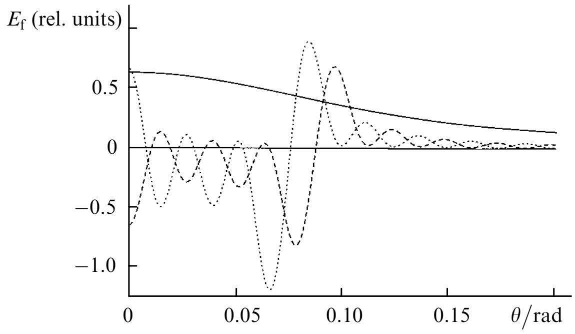

Figure 5. Angular diagrams for the emission of the modes HE_{11} (continuous curve), HE_{17} (dotted curve), and HE_{18} (dashed curve).

Fig. 6 presents the experimental distribution of the far-field intensity obtained on excitation of the mode HE_{17} and also the fitting of the experimental data by the combination of the calculated distributions of the modes HE_{11} and HE_{17} with a phase difference between them ensuring best agreement with experiment. As in the case of measurements by the near-field method, a satisfactory agreement is achieved between the calculated and experimental data, which confirms the validity of the calculation of the distribution of the cladding-mode field.

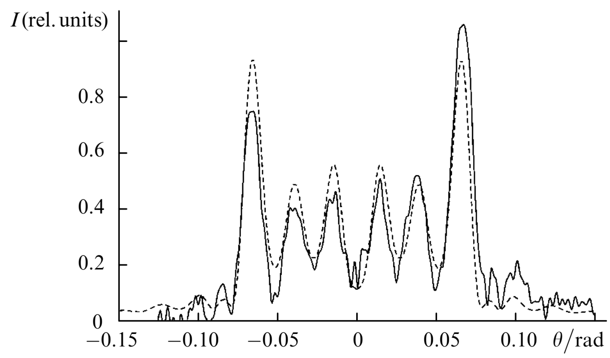

Figure 6. Experimentally measured (continuous curve) and calculated (dashed curve) angular far-field intensity distributions for the combination of the modes HE_{11} and HE_{17}.

5. Propagation of cladding modes

As already mentioned, a fibre RI grating is the best device for the excitation of one mode in a significantly multimode fibre. In an ideal fibre with a constant geometry and isotropic optical properties, the excited mode would propagate without dissipation of its energy, despite the presence of modes with similar propagation constants. In real fibres, there are always different types of inhomogeneities (variations of the RI, diameter, etc. along the fibre axis), on which the propagated radiation is diffracted and hence an intermodal coupling takes place. As a rule, the characteristics of the intermodal coupling in real fibres cannot be calculated because the distribution of the inhomogeneities is unknown, so that experimental studies of the propagation of a grating-excited mode are useful in the investigation of the fibre inhomogeneities.

Fig. 7 illustrates the intermodal coupling in the case of the transformation of the mode HE_{14} into other modes guided by the fibre cladding. The distribution of the near field of the initial mode (the fibre segment located behind the grating is unperturbed) is given on the left, whilst the picture on the right shows the near field when this fibre segment ~ 1 cm long is clamped by a metallic plate with a mass of several grammes. It is readily seen that even a slight transverse stress, arising in the fibre, and/or perturbation of the reflecting outer quartz/air interface can lead to an appreciable intermodal coupling and hence to a virtually complete loss of the initial cladding mode. It may be that Davis et al. [7] observed in a similar experimental geometry a combination of several cladding modes excited by long-period gratings because they underestimated this factor.

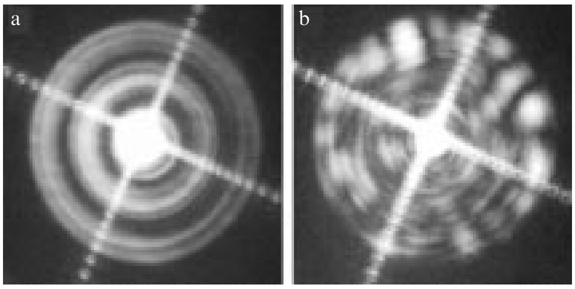

Figure 7. Distribution of the field of the cladding mode measured for the unperturbed end of the fibre (a) and for the end clamped by a metallic plate (b).

In order to measure the possible propagation length of the excited cladding mode along the fibre axis, we determined the distributions of the near field at various points to the rear of the grating. The polymeric cladding was stripped from the fibre behind the grating and, in order to prevent bending of the fibre, the latter was placed in a metal capillary ~ 0.5 mm in diameter. The maximum length of the fibre in the measurements was restricted by the length of the capillary and amounted to 75 cm. It was found that the quality of the image of the investigated cladding mode became impaired as it propagated. Nevertheless, the distribution of the field retained its main features even at the exit from a fibre 75 cm long (Fig. 8), which indicated that an appreciable fraction of the power was again contained in the initial cladding mode.

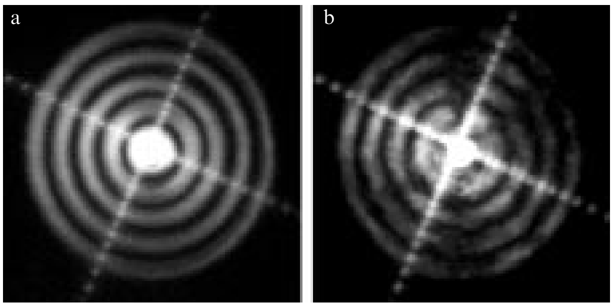

Figure 8. Distribution of the field of the cladding mode obtained for fibre lengths ahead of the grating, of 1 cm (a) and 75 cm (b).

Thus, in a real waveguide the propagation length of an individual cladding mode can reach 1 m under certain conditions. This made it possible to fabricate long gratings and devices containing several gratings distributed along the length of the fibre.

6. Conclusions

The properties of cladding modes excited in long-period fibre RI gratings were investigated by the near- and far-field methods. It was demonstrated experimentally that the modes considered are of the HE_{1m} ($m > 1$) type. A satisfactory agreement between the theoretical and experimental fields of the modes was obtained. It is shown that an individual cladding mode can propagate along a fibre without appreciable loss of energy over distances of the order of 1 m.

Acknowledgements. This work was partly supported by the Russian Foundation for Basic Research (Grant No. 98-02-16807), the Russian Ministry of Science (Project No. 023.03.910/1-96), and the Swiss National Science Foundation (Project No. 7 IP 050160). The authors are indebted to A N Gur'yanov and V F Khopin for making the fibres used in the reported investigation.

References

1. Kashyap R *Opt. Fiber Technol.* **1** 17 (1994)
2. Meltz G, Morey W W, Glenn W H *Opt. Lett.* **14** 823 (1989)
3. Vengsarkar A M, Lemaire P J, Judkins J B, Bhatia V, Erdogan T, Sipe J E *J. Lightwave Technol.* **14** 58 (1996)
4. Erdogan T *J. Lightwave Technol.* **15** 1277 (1998)
5. Vasil'ev S A, Dianov E M, Kurkov A S, Medvedkov O I, Protopopov V N *Kvantovaya Elektron. (Moscow)* **24** 151 (1997) [*Quantum Electron.* **27** 146 (1997)]
6. Erdogan T *J. Opt. Soc. Am. A* **14** 1760 (1997)
7. Davis D D, Gaylord T K, Glytsis E N, Mettler S C *Electron. Lett.* **34** 1416 (1998)
8. Dianov E M, Vasil'ev S A, Kurkov A S, Medvedkov O I, Protopopov V N *Proceedings of the Twenty-Second European Conf. on Optical Communication, ECOC'96, Oslo, 1996* (Kjeller, Norway: Telenor, 1996) Vol. 1, p. 65
9. Gu X J *Opt. Lett.* **23** 509 (1998)
10. Neuman E-G *Single-Mode Fibers — Fundamentals* (Springer Series in Optical Sciences, Vol. 57) (Berlin: Springer, 1998)